

Articles

Structure of Bovine Blood Coagulation Factor Va. Determination of the Subunit Associations, Molecular Weights, and Asymmetries by Analytical Ultracentrifugation[†]

Thomas M. Laue,* Arthur E. Johnson, Charles T. Esmon, and David A. Yphantis

ABSTRACT: Thrombin-activated bovine factor V (factor Va), an essential component of the blood clotting cascade prothrombinase complex, is composed of two nonidentical subunits (V_I and V_h) and Ca²⁺ in tight association. We have examined V_I, V_h, and factor Va using analytical ultracentrifugation. At pH 7.65 in 50 mM tris(hydroxymethyl)aminomethane, 0.1 M NaCl, 1 mM benzamidine, and 10 mM Ca²⁺, the V_I subunit has a molecular weight (M_r) of 82 500, an $s_{20,w}^0 = 5.0_2$ S, and, assuming a model of a prolate ellipsoid with 0.3 g of H₂O/g of protein, an axial ratio of 5:1. The corresponding values for the V_h subunit are an M_r of 92 300, an $s_{20,w}^0 = 5.2_9$ S, and an axial ratio of 5:1. We found these same values for V_I and for V_h in a buffer that contained 2 mM ethylenediaminetetraacetate (EDTA) rather than the 10 mM Ca²⁺. The V_I subunit undergoes a weak, reversible self-association at 9 °C with an apparent monomer-dimer association constant of 5.6×10^3

M⁻¹ in the presence of 2 mM EDTA and 2.3×10^3 M⁻¹ in the presence of 10 mM Ca²⁺. Our data indicate that the V_I self-association includes dimer and higher oligomers. Factor Va, examined in the presence of 10 mM Ca²⁺ and at 20 °C, has an M_r of 174 000, an $s_{20,w}^0 = 8.1_8$ S, an axial ratio of 5:1, and an apparent V_I-V_h association constant of at least 2.7×10^8 M⁻¹. Our results suggest that factor Va self-associates to form higher multimers. When solutions of Va are dialyzed against a buffer that contains no Ca²⁺ and 2 mM EDTA, the apparent V_I-V_h subunit association constant is reduced to 9.4×10^3 M⁻¹. Our hydrodynamic data indicate that there is a substantial decrease in molecular asymmetry when factor V is proteolytically activated by thrombin to form factor Va and that V_I and V_h are arranged "side by side" rather than "end to end" in factor Va.

Factor Va is an essential component of the blood clotting cascade prothrombinase complex. Factor Va appears to function in this complex as a protein cofactor that accelerates the conversion of prothrombin to thrombin by the protease factor Xa (Davie & Fujikawa, 1975; Jackson & Nemerson, 1980). Factor Va is produced from its high molecular weight

precursor, factor V, through a series of discrete proteolytic cleavages by thrombin (Nesheim et al., 1979a; Esmon, 1979; Dahlback, 1980; Rosing et al., 1980; Kane & Majerus, 1981). Work by Nesheim et al. (1979a) has characterized factor V as being a large (M_r 330 000) and asymmetric (prolate axial ratio of 25:1) single-chain glycoprotein. The recent availability of highly purified factor Va (Nesheim et al., 1979a; Esmon, 1979) makes it possible to explore its structure in detail.

It has been established that factor Va has an equimolar ratio of two nonidentical subunits (V_I and V_h) that are held together by noncovalent bonds (Nesheim & Mann, 1979; Esmon, 1979; Guinto & Esmon, 1982). Guinto & Esmon (1982) have reported one Ca²⁺ binding site (apparent $K_d = 24 \mu\text{M}$) per mole of subunits in Va. Neither the V_I subunit nor the V_h subunit alone exhibits significant affinity for Ca²⁺ (Guinto & Esmon, 1982), which suggests that the V_I-V_h association and the formation of the high-affinity Ca²⁺ binding site in factor Va are strongly linked.

In this investigation, we have used sedimentation equilibrium and sedimentation velocity techniques to determine molecular

[†] From the Department of Chemistry, University of Oklahoma, Norman, Oklahoma 73019 (T.M.L. and A.E.J.), the Section of Hematology and Thrombosis, Oklahoma Medical Research Foundation, Oklahoma City, Oklahoma 73104 (C.T.E.), the Departments of Pathology and Biochemistry, University of Oklahoma Health Sciences Center, Oklahoma City, Oklahoma 73190 (C.T.E.), and the Biochemistry and Biophysics Section, Biological Sciences Group, University of Connecticut, Storrs, Connecticut 06268 (D.A.Y.). Received July 28, 1983. This work has been supported in part by a fellowship from the Oklahoma affiliate of the American Heart Association (to T.M.L.), by Grant 81-1189 from the American Heart Association with funds contributed in part by the Oklahoma affiliate (to A.E.J.), by National Institutes of Health Grants P01 HL30073 and R01 HL29807 (to C.T.E.), by an Established Investigatorship of the American Heart Association with funds contributed in part by the Oklahoma affiliate (to C.T.E.), and by National Science Foundation Grant 81-11484 (to D.A.Y.).

weights, association constants, hydrodynamic parameters, apparent sizes, and asymmetries for VI, Vh, and factor Va. The subunit interactions have been examined in the presence of ethylenediaminetetraacetate (EDTA)¹ and in the presence of saturating levels of Ca²⁺ in order to assess the linkage between Ca²⁺ binding and subunit association (Weber, 1975).

Materials and Methods

Protein Preparation. Factor Va preparation and the isolation of the VI and Vh subunits from factor Va were performed as described by Esmon (1979). Factor V activity was measured by a one-stage clotting assay (Esmon, 1979). Protein fractions were chosen for sedimentation analysis on the basis of homogeneity as examined by sodium dodecyl sulfate–polyacrylamide electrophoresis [7.5% resolving gel, as described by Laemmli (1970)]. The following additions to the published isolation procedure were included to prevent sample degradation during the experiments. The pooled factor V solution was made 20 μ M with (*p*-amidinophenyl)methanesulfonyl fluoride protease inhibitor prior to thrombin activation. The chromatographic column fractions of Va, VI, or Vh chosen for analysis were pooled, made 1 mM in DFP, brought to a final protein concentration of about 0.1% (by using either a Minicon B-15 or a Millipore CX-30 concentrator), again made 1 mM in DFP, split into two samples of equal volume, and dialyzed. Dialysis was performed for 72 h at 4 °C with slow stirring against three changes (1000:1 v/v) of buffer [0.1 M NaCl, 0.05 M Tris (pH 7.65), and 1 mM benzamidine, hereafter called buffer A] containing either 2 mM EDTA or 10 mM CaCl₂. Samples were kept in sterile capped plastic tubes at 4 °C until used (within 2 weeks of the final dialysis). Protein integrity was checked both before and after centrifugation experiments by using sodium dodecyl sulfate–polyacrylamide gel electrophoresis.

Partial Specific Volume. The partial specific volumes (\bar{v}) of the proteins were calculated from the amino acid and carbohydrate compositions given by Guinto & Esmon (1982) according to the method of McMeekin & Marshall (1952). The values of \bar{v} were estimated for the various individual carbohydrate types from their structures by using the method outlined in Cohn & Edsall (1943). The calculated values were $\bar{v}(\text{VI}) = 0.717 \text{ cm}^3/\text{g}$, $\bar{v}(\text{Vh}) = 0.720 \text{ cm}^3/\text{g}$, and $\bar{v}(\text{Va}) = 0.719 \text{ cm}^3/\text{g}$.

Sedimentation Velocity. Sedimentation velocity experiments were performed with a Beckman Model E analytical ultracentrifuge at speeds of 52 000 or 60 000 rpm and at a constant temperature between 21 and 25 °C. The experiments were carried out over a protein concentration range from 0.07 to 0.3% (VI, Vh, or factor Va in 2 mM EDTA) or from 0.07 to 0.54% (factor Va in 10 mM Ca²⁺) using a 12-mm double-sector centerpiece and schlieren optics. The solvent sector was filled with dialysate from the final step of the protein preparation. Photographs were made on Kodak Ortho film (Paul & Yphantis, 1972).

The radial position of the schlieren peak was determined with a Nikon 6C comparator from 10–15 photographs made at 8-min intervals during the run. Apparent sedimentation coefficients were determined by linear regression analysis of the logarithm of the peak position as a function of time. The sedimentation coefficients were corrected to standard conditions (water at 20.0 °C) using the formulation given by

Schachman (1959) and tabulated density and viscosity data (Washburn, 1928; Weast, 1968). $s_{20,w}^0$ was obtained by extrapolation of the $s_{20,w}$ data to zero protein concentration. The frictional coefficient ratios (f/f_{min}) for VI, Vh, and Va were calculated from their molecular weights, partial specific volumes, and sedimentation coefficients by using the formulation of Oncley (1941). These f/f_{min} ratios were used to calculate values of the Perrin shape factor (f/f_0) at each of several degrees of hydration by using eq 21–28 given by Tanford (1961). The axial ratio (a/b) of the prolate ellipsoid of revolution that corresponded to a given value of f/f_0 was read from a plot of f/f_0 vs. a/b made by using the data in Table 10-2 of Cantor & Schimmel (1980).

Sedimentation Equilibrium. Sedimentation equilibrium measurements were made by using the “meniscus-depletion” method (Yphantis, 1964). The experiments were conducted with a Beckman Model E analytical ultracentrifuge equipped with Rayleigh interference optics, a pulsed argon ion laser light source (Paul & Yphantis, 1972), a bulk film camera modified to use 150-ft rolls of 35-mm film (Kodak 2415 Technical), and a minicomputer to operate the light source and camera (Laue, 1981). Either an AN-J or an AN-F-Ti (for speeds >18 000 rpm) four-place rotor was used. The rotor temperature was regulated at either 20.0 or 9.0 °C. Two “externally loaded” cells (Ansevin et al., 1970), with three pairs of solution–solvent channels per cell (3 mm high and 12 mm thick) and with sapphire windows, were used in each experiment. The reference solvent was the dialysate from the final step of the protein preparation.

A 350- μ L aliquot of the protein solution was spun for 5 min in a Beckman 152 microfuge to remove any large particulates. Then serial dilutions were made (typically 1:2, 1:4 or 1:3, 1:9 by volume). The diluted samples were spun again for 5 min in the microfuge just before the cell was loaded.

The solutions containing the isolated VI or Vh subunits were analyzed at speeds of 18 000, 22 000, and 26 000 rpm. The solutions of factor Va were analyzed at 15 000 rpm. Sufficient time was allowed at each speed for equilibrium to be reached by the criteria of Van Holde & Baldwin (1958). Three or four interferogram exposure series were made at 2–10-h intervals following the estimated equilibration time. Blank interferograms were obtained before and after each experiment following the procedure previously described (Yphantis, 1964). Fringe displacement data from over 450 channels were obtained at a radial spacing of 10 μ m in the magnified cell image (corresponding to 4 μ m in the cell coordinates) by using an automated photographic plate reader (Laue & Yphantis, 1979; Laue, 1981). The fringe displacements were calculated from the “phase” of a Walsh transform taken over a portion of the total fringe envelope (typically three fringes) at each radial position (Laue & Yphantis, 1979). The data were edited by using the XEQ program (Correia, 1981) and stored on magnetic tape. In order to prevent Wiener skewing from affecting our data at high concentration gradients, the data were truncated to exclude fringe gradients above 15 mm/cm² determined as a function of $r^2/2$; this corresponds to 375 fringes/cm at a radius of 6.5 cm in the solution.

Data Analysis. The edited, blank corrected fringe displacements were analyzed by two computer programs, BIOSPIN and NONLIN. BIOSPIN was used to calculate the local (point) reduced weight-average molecular weight as a function of concentration, σ_w , as defined by Yphantis (1964) and implemented by Roark & Yphantis (1969). $M_w(c)$ was calculated from σ_w as described below. The superposition of graphs of the concentration dependence of $M_w(c)$ from experiments at

¹ Abbreviations: EDTA, ethylenediaminetetraacetate; DFP, diisopropyl fluorophosphate; Tris, tris(hydroxymethyl)aminomethane; rms, root mean square; rpm, revolutions per minute; $M_w(c)$, concentration-dependent apparent local (point) weight-average molecular weight.

different protein loading concentrations and at different speeds was used as a diagnostic of solution homogeneity (Squire & Li, 1961; Roark & Yphantis, 1969; Yphantis et al., 1978). Typically, more than 200 determinations of $M_w(c)$, each with an estimated precision of measurement better than 3%, were made for each data set. For the sake of clarity, only about 10% of the total number of points from each data set are shown in Figures 2 and 3. These graphs provide direct information about the nature of a system. However, it is difficult to obtain precise quantitative information regarding the stoichiometries and association constants from these point-average determinations (Roark & Yphantis, 1969; Teller, 1973; Johnson et al., 1981).

NONLIN performs a simultaneous nonlinear least-squares fit of one or more channels of ultracentrifuge data at different loading concentrations, radial positions, and possible angular velocities to specific association and/or nonideality schemes (Johnson et al., 1981). It also can fit data that span a pre-selected concentration range. This permitted us to exclude the highest or the lowest fringe displacement data points or to fit data from channels at different loading concentrations over a common concentration range. The program returns values and confidence intervals for the fitted parameters (e.g., the reduced monomer molecular weight, the second virial coefficient, and association constants). The confidence limits reported here (in parentheses, Tables I–V) correspond to the 65% confidence interval. These confidence intervals reflect the precision of the fit of a particular model to the experimental data and do not necessarily reflect the accuracy of the determination.

While the "whole system" approach of NONLIN is far more precise and is considerably less sensitive to local optical aberrations than the point-average method of BIOSPIN, it does not provide *direct* information about the system. Therefore, the simplest models that adequately fit our experimental data were used to obtain the values presented here. More complex schemes (i.e., ones with more fitting parameters) were considered useful and necessary only if they significantly decreased variance and improved the "goodness of fit" as judged by the criteria outlined by Johnson et al. (1981).

Concentration Determination and Conversion of Units. Protein concentration was estimated from the absorbance at 280 nm. The extinction coefficients (E) used for Va, V1, and Vh were 15.1, 18.7, and 12.9 %⁻¹ cm⁻¹, respectively (Guinto & Esmon, 1982). Conversion from the fringe displacement concentration scale to other concentration scales was made by using a protein refractive increment of 0.19 mL/g (at 514.5 nm). This refractive increment was based on the tabulated values for proteins with similar amino acid compositions and under similar conditions (Sober, 1970).

The values of σ returned by BIOSPIN and NONLIN were converted to their corresponding molecular weights from the definition of σ (Yphantis & Waugh, 1956; Yphantis, 1964) using the values for the partial specific volumes listed previously and solvent densities calculated for the buffer composition and temperature.

The molar association constants were determined from the best-fit values of the respective $\ln K_i$ (i = degree of association) from NONLIN. The units of K_i were converted from reciprocal fringe displacement units (inverse millimeters to the $i - 1$ power) to reciprocal molarity units (1/M to the $i - 1$ power) by using the best-fit molecular weight for each case and a protein refractive increment of 0.19 mL/g. For self-associating systems:

$$K_{i,M} = K_{i,mm}(M_a^{i-1}/i)(Y_T/C_T)^{i-1} \quad (1)$$

where $K_{i,M}$ is the association constant on the molar concentration scale, $K_{i,mm}$ is the association constant on the millimeters of fringe displacement concentration scale, M_a is the monomer molecular weight, and Y_T/C_T is the specific fringe displacement [0.849 (mm·L)/g for the experiments reported here]. For an (A + B)-type association, the corresponding equation is

$$K_{i,M} = K_{i,mm}(M_a M_b / M_{ab})(Y_T/C_T) \quad (2)$$

where M_a , M_b , and M_{ab} are the molecular weights of A, B, and the AB complex, respectively.

Interpretation of Apparent Dimer Formation Constants. For some experiments involving factor Va, we have analyzed the data as though we were examining an ideal monomer-dimer equilibrium with a hypothetical monomer with a molecular weight of 87 100 (the approximate weight-average molecular weight of an equimolar mixture of the V1 and Vh subunits). The apparent dimer formation constant (K_1) in these analyses (at concentrations where no polymer larger than a dimer is formed) is determined as

$$K_1 = ([VIVh] + [VIVl])/([Vl] + [Vh])^2 \quad (3)$$

where [VIVh] is the concentration of the VIVh complex (either with or without Ca²⁺), [VIVh] is the concentration of the dimer formed by the V1 subunit, and [Vl] and [Vh] are the free concentrations of the light and heavy subunits, respectively. In order to estimate K_{VIVh} , the V1 to Vh association constant, it is necessary to correct K_1 for the V1 subunit self-association that we observed and quantitated in other experiments. To do this, we assume that throughout the cell [Vl] = [Vh]. Implicit in this assumption are the requirements that there be no fractionation of the subunits by the gravitational field and that [VIVl] be small. The latter restriction is met in these experiments by the small value of K_{V12} . Substitution for the associated species in terms of their formation constants and the free monomer concentration (2[Vl]) gives the formation constant for the VIVh complex as

$$K_{VIVh} = 4K_1 - K_{V12} \quad (4)$$

where K_{VIVh} is the formation constant for the VIVh complex and K_{V12} is the V1 subunit dimer formation constant that is determined from separate experiments.

Synthetic Data. Data were generated to simulate the concentration dependence of the point-average σ_w , on the basis of the fitting parameters returned by NONLIN (Johnson et al., 1981). We assumed a meniscus positioned radially at 6.4 cm, the cell base at 6.7 cm, and a cell loading concentration that approximated the particular experiment being modeled. $M_w(c)$ was calculated from the point-average σ_w as described above.

Estimates of the Second Virial Coefficient. Estimates of the second virial coefficient were made from the sum of the approximate excluded volume contributions (assuming either spherical molecules or rods with $1/d = 5$) and the charge contributions using equations given in Tanford (1961). The macromolecular charge was estimated from the amino acid composition and the approximate subunit isoelectric pHs (V1, pH 7.0–7.5; Vh, pH 5.0–5.5; Guinto, 1983) under the assumption that only the histidine residues (assumed $pK_a = 7.0$) titrated in the pH 5.0–7.5 range. The charge was estimated to be between 15– and 20– on the Vh subunit and between 0 and 5– on the V1 subunit. The estimated second virial coefficient in buffer A is $(4-5) \times 10^{-5}$ mol·cm³·g⁻² for the V1 subunit and $(5-10) \times 10^{-5}$ mol·cm³·g⁻² for the Vh subunit, where the ranges encompass the extremes implied by the assumptions.

Table I: Monomer Molecular Weight and Apparent Monomer-Dimer Association Constant for the Bovine Factor Va Light Subunit (VI)

solution	speed (rpm)	monomer mol wt	app dimerization constant (M^{-1})	max fringe displacement used (mm) ^a	rms of variance (μm) ^b
EDTA, 9 °C	22 000	82 900 (81 800–84 000)	5600 (4700–6700)	1.72, 1.45, 0.97	3.80
	26 000	82 600 (81 600–83 400)	6150 (5300–7400)	1.43, 1.34, 1.02	3.59
Ca^{2+} , 9 °C	22 000	82 100 (80 800–83 400)	2700 (2200–3400)	2.48, 0.47	3.68
	26 000	82 200 (80 900–83 400)	1900 (1300–2900)	1.62, 0.49	4.60

^a Maximum fringe displacement of each of the channels used in the simultaneous fit corresponding to 0.18%, 0.06%, and 0.02% (EDTA) or 0.18% and 0.018% (Ca^{2+}) protein loading concentrations. ^b Root mean square of variance for the nonlinear fit.

Table II: VI Subunit at 18 000 rpm and 9 °C in 2 mM EDTA: Fits to Different Ideal Association Schemes^a

	monomer	monomer-dimer	monomer-dimer-trimer	monomer-dimer-tetramer
monomer mol wt	96 900 (95 700–98 400)	77 300 (75 500–79 200)	83 200 (82 300–84 100)	82 000 (80 600–83 400)
K_2 (M^{-1})		13 000 (11 000–16 000)	3500 (2600–4300)	5900 (4800–7200)
K_3 (M^{-2})			6.3×10^7 (6.1×10^7 – 6.4×10^7)	
K_4 (M^{-3})				1.0×10^{12} (0.9×10^{12} – 1.1×10^{12})
rms ^b (μm)	12.6	4.53	3.88	3.85

^a Simultaneous fit of three channels with loading concentrations of 0.18%, 0.06%, and 0.02% with maximum fringe displacements of 2.64, 2.20, and 0.72 mm, respectively. ^b Root mean square of variance for the nonlinear fit.

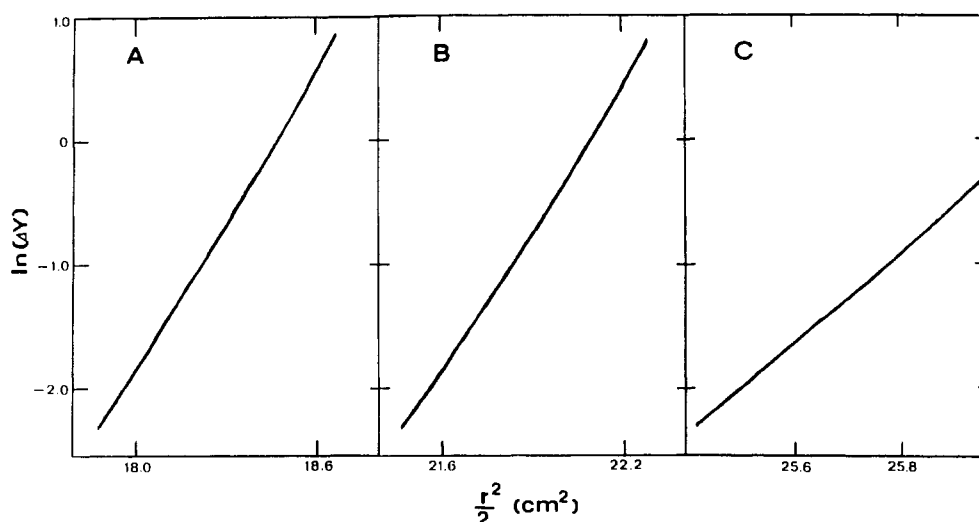


FIGURE 1: Sedimentation equilibrium data at 18 000 rpm for the VI subunit plotted as the natural logarithm of the fringe displacement as a function of $r^2/2$. These data are from experiments performed at 9 °C and in buffer A that contained 2 mM EDTA. The three panels present the data from channels at three protein loading concentrations: (A) 0.18%; (B) 0.06%; (C) 0.03%. The graph in each panel is composed of points from blank-corrected fringe displacements measured at 300–400 radial positions.

Results and Discussion

Factor VI Subunit Monomer Molecular Weight. The VI monomer molecular weights, determined for various ideal association models (see below), are presented in Tables I and II. The average value for the monomer molecular weight, 82 500, as determined from the best-fit models, was constant to within 1.3% for data taken at three different rotor speeds, for three different protein loading concentrations, and for buffer that contained either 2 mM EDTA or 10 mM Ca^{2+} . The apparent molecular weights reported for VI from analyses by polyacrylamide gel electrophoresis in the presence of sodium dodecyl sulfate (73 000–81 000; Nesheim & Mann, 1979; Guinto & Esmon, 1982) are consistent with our value for the

VI monomer molecular weight.

Evidence for VI Self-Association. There is compelling evidence that the VI subunit undergoes a weak, reversible self-association, even in the absence of Ca^{2+} . Careful inspection of the graphs in Figure 1 shows that there is a positive curvature to the plots. The apparent molecular weights calculated from the best-fit slopes of these plots are 104 700 (Figure 1A), 98 500 (Figure 1B), and 94 300 (Figure 1C). Graphs of $M_w(c)$ for these solutions exhibit nearly the same concentration dependence in experiments conducted at three different protein loading concentrations (Figure 2A) and for a sample analyzed at three different rotor speeds (Figure 2B). Nonlinear least-squares analysis indicates that there is at least a 3.5-fold decrease in the variance of the fit when models that

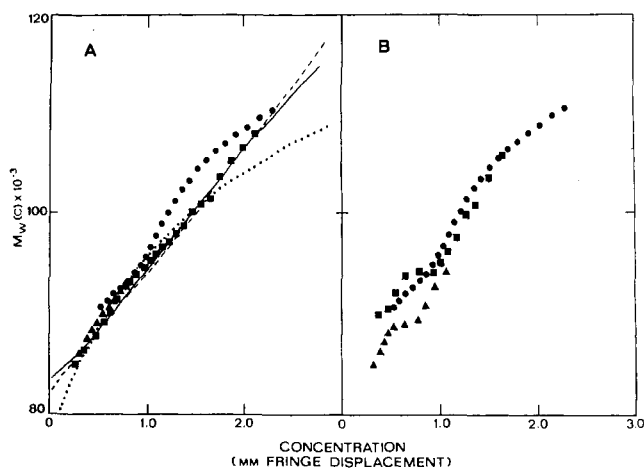


FIGURE 2: Concentration dependence of $M_w(c)$ for the VI subunit. The data for both panels are from experiments that examined solutions of the VI subunit at 9 °C in buffer A containing 2 mM EDTA. (A) $M_w(c)$ values from experiments performed at three different protein loading concentrations have been determined by BIOSPIN (Materials and Methods) and are presented here as a function of the observation concentrations. One millimeter of fringe displacement corresponds to a concentration of about 1 g/L. Individual data points from channels with protein loading concentrations of (●) 0.18%, (■) 0.06%, and (▲) 0.03% are shown here. The three curves were generated from the best-fit monomer molecular weights and equilibrium constants given in Table II for the monomer-dimer model (dotted line), the monomer-dimer-trimer model (dashed line), and the monomer-dimer-tetramer model (solid line). (B) concentration dependence of $M_w(c)$ for solutions of the VI subunit analyzed at three speeds: 18 000 rpm (●); 22 000 rpm (■); 26 000 rpm (▲). The protein loading concentration for each experiment was 0.18%.

include self-association are compared with that for a single ideal thermodynamic component (Table II). These observations are consistent with the behavior expected for a reversibly associating system and are inconsistent with the behavior expected for a system exhibiting simple molecular weight heterogeneity (Squire & Li, 1961; Yphantis, 1964; Roark & Yphantis, 1969; Yphantis et al., 1978).

Consideration of a VI Monomer-Dimer Equilibrium. For experiments conducted in 2 mM EDTA at 22 000 or 26 000 rpm, the maximum usable fringe displacement was 1.72 mm, which corresponds to a maximum protein concentration of 20 μ M. We could adequately fit individual channels of data, or, as presented in Table I, we could simultaneously fit the data for the three loading concentrations as an ideal monomer-dimer equilibrium with an apparent association constant near 5600 M^{-1} . There was at least a 1.5-fold decrease in the variance when the fit by this model was compared with the fit obtained for a model consisting of an ideal single thermodynamic component (data not shown). Other association schemes that were tested (e.g., monomer-trimer, monomer-tetramer, monomer-dimer-trimer, etc.) provided no significant improvement in the fit to the data (data not shown). When we included our estimate of the nonideality into the model used to fit the data, there was no improvement in the variance of the fit, the monomer molecular weight remained unchanged (within 0.2%), and the apparent association constant increased to 6300 M^{-1} .

VI self-association also occurs in the presence of 10 mM Ca^{2+} . There was a significant improvement in the fit (a 1.4-fold decrease in the root mean square of the fit) when these data were analyzed as an ideal monomer-dimer equilibrium rather than as an ideal nonassociating system (data not shown). The apparent monomer-dimer association constant determined from data taken at two different protein loading concentrations and at two different speeds was about 2300 M^{-1} (Table I).

Graphs of $M_w(c)$ indicated that these solutions were homogeneous (data not shown). These data were modeled adequately by the ideal monomer-dimer association scheme over the entire concentration range examined (up to 25 μ M). Other association schemes that were considered (see above) provided no significant improvement in the fit to the data. When we included our estimate of the nonideality into the monomer-dimer equilibrium model, there was no improvement in the variance of the fit, the monomer molecular weight remained unchanged (within 0.1%), and the apparent association constant increased somewhat from 2300 to 2700 M^{-1} .

Evidence for VI Self-Association Past the Dimer Form. The data for VI in buffer A containing 2 mM EDTA and sedimented at 18 000 rpm examined the association behavior of the VI subunit over a broader protein concentration range (up to 28 μ M) than the experiments at 22 000 or 26 000 rpm. At a low protein loading concentration (0.02%, maximum fringe displacement of 0.78 mm), the data modeled well as an ideal monomer-dimer equilibrium with a monomer molecular weight (81 500) and an apparent dimer formation constant (5200 M^{-1}) that were consistent with the values presented in Table I. However, the data from experiments at higher protein loading concentrations (0.06% or 0.18%, maximum usable fringe displacements of 2.20 and 2.64 mm, respectively) were not fit well by this model (Table II, Figure 2A). When these last two data sets were truncated so as to include only fringe displacements less than 1000 μ m, the apparent monomer molecular weight (81 800), the apparent dimer formation constant (7400 M^{-1}), and the fit ($rms = 3.40 \mu$ m) were in good agreement with the values presented in Table I. We believe, therefore, that the higher molecular weight species observed in these experiments represent higher oligomers of the VI subunit that are in equilibrium with the VI monomer and do not simply reflect the presence of nonequilibrating high molecular weight contaminants.

Stoichiometry of the Higher Oligomers of VI. We have analyzed the 18 000 rpm data using several models that could account for the presence of higher oligomers of VI. Models that considered a VI monomer in equilibrium with only a single higher polymer (monomer- n -mer, where $n = 3, 4, \dots, 8$) provided a poor fit to the data (data not shown). Instead, the data were best fit by models that included dimerization and association past the dimer. The best-fit data for two models of this sort (monomer-dimer-trimer and monomer-dimer-tetramer) are presented in Table II and Figure 2A. Note that the monomer molecular weights and dimer formation constants determined with these two models are consistent with those presented in Table I. Note, too, that we are unable to designate one of these two models as being uniquely correct either on the basis of the root mean square of their fits (Table II) or by a comparison of their relative abilities to account for the concentration dependence of $M_w(c)$ (Figure 2A). The relative strengths of the dimer and trimer formation constants (Table II) suggest that VI may undergo an isodesmic association under these conditions. Indeed, these data could be fit ($rms = 3.56 \mu$ m) by a model that considered a monomer (M_w 82 500) in equilibrium with all oligomers through a decamer, with an isodesmic association constant of 5600 M^{-1} . However, the relatively low degree of association at the highest concentrations observed in these experiments (less than 15% for the most extreme possibility, a trimer) makes it impossible to assign a unique and unambiguous association scheme for VI, past that of the dimer (Teller, 1973).

Factor Vh Subunit Molecular Weight. The average value found for the Vh subunit molecular weight, 92 300 (Table III),

Table III: Molecular Weight of the Bovine Factor Va Heavy Subunit (Vh)

solution	speed (rpm)	app mol wt ^a	loading concn used for fit (%)	max fringe displacement after truncation (mm) ^b	rms of variance (μm) ^c
EDTA, 20.0 °C	18 000	93 500 (92 800–94 300)	0.09, 0.045	0.998	3.01
	22 000	90 100 (89 100–91 000)	0.09, 0.045	0.998	4.71
EDTA, 9.0 °C	18 000	93 100 (92 200–93 900)	0.05, 0.017	1.97	5.57
	22 000	93 700 (93 100–94 400)	0.05, 0.017	1.98	4.76
	26 000	91 180 (89 940–91 800)	0.05, 0.017	1.99	4.63
	22 000	91 800 (90 900–92 700)	0.04	0.994	4.00

^a When fit as a single ideal species using truncated data sets; see text for details. ^b Data sets used for simultaneous fit were edited so as to exclude fringe displacements greater than values given in this column; see text for details. ^c Root mean square of the variance of the non-linear fit to the truncated data sets.

was determined from truncated fringe displacement data (see below) that were fit to a model of an ideal single thermodynamic species. The value was constant to within 3.8% for determinations made at three different rotor speeds, at six different protein loading concentrations, at two temperatures, and in buffer containing either 2 mM EDTA or 10 mM Ca^{2+} . The M_r of 94 000 reported for the Vh subunit from sodium dodecyl sulfate gel electrophoresis analysis (Nesheim & Mann, 1979; Guinto & Esmon, 1982) is in agreement with our value.

When we fit *untruncated* fringe displacement data to a model of a single thermodynamically ideal macromolecular species (data not shown), we observed a slight increase (0–4%, depending on the particular data sets examined) in the apparent molecular weight with decreased cell loading concentration, suggesting the presence of nonequilibrating higher molecular weight contaminants (Yphantis, 1964). Accordingly, the molecular weights presented in Table III were obtained from data sets that were systematically truncated at total fringe displacements of 2000, 1500, 1000, 750, and 500 μm so that the contributions of heavier material to the determination were minimized. Over a complete set of truncations, the fitted molecular weight was never reduced by more than 2.5%, but the variance of the fit was improved by as much as 25%.

Molecular Weight and Subunit Stoichiometry in Factor Va. The $M_w(c)$ data for solutions of factor Va, analyzed at three total protein loading concentrations and in a buffer containing 10 mM Ca^{2+} , are shown in Figure 3. Assays on these samples showed that they had over 400 units/ A_{280} of factor V activity. Over nearly the entire concentration range examined, the apparent weight-average molecular weight for these solutions is within the confidence limits of the simple sum of the molecular weights of one VI subunit and one Vh subunit in tight association. Therefore, we will use the name Va when referring to the Ca^{2+} -containing complex consisting of 1VI:1Vh.

Consideration of Two Distinct Equilibria in Va Solutions. Analysis of individual channels of data as an ideal single thermodynamic component reveals that the apparent molecular weight (M_{app}) increases with increased protein loading concentration (M_{app} 169 800 at 0.032%, M_{app} 178 700 at 0.065%, and M_{app} 180 100 at 0.13%). The near-coincidence of the concentration dependence of $M_w(c)$ for these channels (Figure 3) suggests the presence of reversible equilibria (Yphantis, 1964). However, over the full concentration range examined, we were unable to fit our data to any model that consisted of

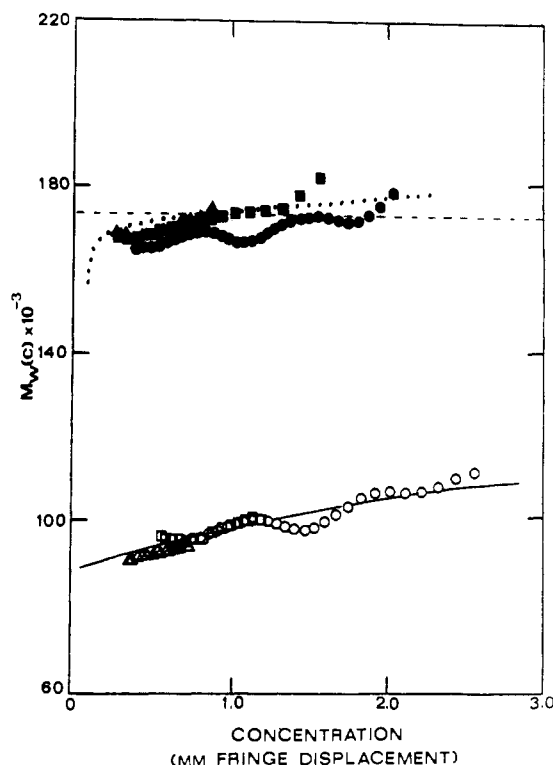


FIGURE 3: Concentration dependence of $M_w(c)$ for factor Va. Solutions of factor Va were examined in a solvent consisting of buffer A that contained either 10 mM Ca^{2+} (closed symbols) or 2 mM EDTA (open symbols). The experiments were carried out at 15 000 rpm and at 20 °C. For either solvent condition, the data from experiments at three protein loading concentration are shown: 0.13% (circles); 0.065% (squares); 0.032% (triangles). The models used to obtain the data for the solid line and the dotted line are described in the text. The dashed line is drawn at 174 800, the molecular weight expected for a VI-Vh complex from the simple sum of the subunit molecular weights.

a monomer in equilibrium with a *single* higher polymer (monomer-*n*-mer, $n = 1-8$). Thus, it appears that at least two association equilibria should be considered.

We have analyzed our data for a model that considers two equilibria: (1) a strong VI-Vh association, characterized by the association constant K_{VI-Vh} , to form a Va molecule and (2) a weak association of Va to form higher multimers. Estimates of the two equilibrium constants in this model were made from analyses of the macromolecular association behavior observed

Table IV: Factor Va Examined in 10 mM Ca^{2+} at 20 °C and 15 000 rpm; Fits to Different Ideal Association Schemes^a

model used for analysis ^b	concn range (mm) ^c	monomer mol wt	app association constants			rms (μm) ^d
			K_1 (M^{-1})	K_2 (M^{-2})	K_3 (M^{-3})	
monomer-dimer	0.000–0.994	87 100 ^e	6.7×10^7			4.27
monomer-dimer	0.204–1.876	174 200 ^e	$(5.5 \times 10^7 - 7.2 \times 10^7)$			5.36
monomer-dimer-trimer	0.000–2.918	87 100 ^e	3100 (2300–4000)	12×10^{12} (10×10^{12} – 14×10^{12})		5.49
monomer-dimer-tetramer	0.000–2.918	87 100 ^e	6.7×10^7 ^e		12×10^{18} (10×10^{18} – 13×10^{18})	4.86

^a Simultaneous fit of three channels with protein loading concentrations of 0.13%, 0.065%, and 0.032% and maximum observed fringe displacements of 2.918, 1.876, and 0.876 mm, respectively. ^b Stoichiometry of the model used to fit to the data. ^c The data sets were edited so as to exclude any points with fringe displacements outside of the indicated range prior to analysis. ^d Root mean square of the variance for the nonlinear fit. ^e Value held constant during nonlinear fit.

over different protein concentration ranges (Table IV). Because the two associations differ in strength by over 4 orders or magnitude (Table IV), it is unnecessary to correct the apparent equilibrium constants for the presence of the second association.

VI-Vh Affinity in Va. $K_{\text{VI-Vh}}$ was calculated as described under Materials and Methods from the apparent K_1 determined for data sets in which the maximum fringe displacement was truncated at 1.0 mm (Table IV). The value of $K_{\text{VI-Vh}}$ systematically increased about 5% as the maximum fringe displacement included in the data set used to determine K_1 was increased from 0.75 to 1.50 mm (data not shown). For $K_1 = 6.7 \times 10^7 \text{ M}^{-1}$ (Table IV) and $K_{\text{V12}} = 2300 \text{ M}^{-1}$, we calculate that $K_{\text{VI-Vh}} = 2.7 \times 10^8 \text{ M}^{-1}$ by using eq 4. The contribution of K_{V12} (determined at 9 °C) to $K_{\text{VI-Vh}}$ (determined at 20 °C) is negligibly small, so that we may safely neglect differences in K_{V12} due to the temperature. Note that only 2–3% of the total protein is in the form of the free subunits at a concentration corresponding in 100 μm of fringe displacement. Since this is the lowest concentration examined by BIOSPIN, we do not expect to see a significant decrease in $M_w(c)$ in Figure 3.

The value for $K_{\text{VI-Vh}}$ determined here probably represents a lower limit for the true value of $K_{\text{VI-Vh}}$. It is likely that heterogeneity described as “incompetent monomer” (Yphantis et al., 1978) could occur in these solutions, both as a result of proteolytic damage to the subunits and as a result of non-equivalence of the subunit concentrations. Heterogeneity of this sort can strongly influence the apparent association constant determined in this type of experiment (Teller et al., 1969; Yphantis et al., 1978). For example, a contamination of only 2%, under the conditions of these experiments, would result in an underestimate of the value of $K_{\text{VI-Vh}}$ by an order of magnitude or more.

Va Self-Association. The data were fit adequately over the full concentration range as an ideal monomer-dimer-higher polymer system when we fixed the monomer molecular weight at 87 100 and the apparent dimer formation constant at $6.7 \times 10^7 \text{ M}^{-1}$. We wished to determine the stoichiometry of the higher polymer and, in particular, whether it was best represented as a trimer (e.g., 2V1:1Vh or 1V1:2Vh) or as a tetramer (e.g., 2V1:2Vh or 3V1:1Vh). The results presented in Table IV suggest that the monomer-dimer-tetramer model provided a better fit (a 12% decrease in the root mean square of the deviations of the fit when compared with the monomer-dimer-trimer model) to our data. Moreover, use of the monomer-dimer-trimer model resulted in residuals of the fit (data not shown) that exhibited systematic deviations consistent with an underestimate of the stoichiometry of the association. Models that considered other stoichiometries (e.g.,

monomer-dimer-hexamer) or more complex association schemes (e.g., monomer-dimer-trimer-tetramer) did not provide significantly better fits to our data. We believe, then, that the weak association we observe results from an association of Va molecules form higher multimers. Although we were not able to assign an unambiguous and unique stoichiometry to the association, our data are consistent with the formation of a 2V1:2Vh species. The dotted line in Figure 3 is drawn for synthesized data based on the parameters for the monomer-dimer-tetramer model in Table IV.

A direct estimate of the Va dimer formation constant was made from data sets that were truncated at a minimum fringe displacement of 0.2 mm and then fit to a model of an ideal monomer-dimer equilibrium with the monomer molecular weight fixed at 174 200 (Table IV). The value obtained by this method (3100 M^{-1}) is consistent with the value of K_3 determined by using a monomer-dimer-tetramer model to fit the entire data set (Table IV). This apparent dimer formation constant exhibited a small systematic increase (from 2200 to 3200 M^{-1}) as the minimum fringe displacement included in the data sets was increased systematically from 0.050 to 0.250 mm.

VI-Vh Association in the Absence of Ca^{2+} . The $M_w(c)$ data from experiments that examined factor Va in buffer A containing 2 mM EDTA are presented in Figure 3 (open symbols). Extrapolation of these data to zero protein concentration gives an apparent molecular weight of 85 000–90 000, the approximate weight-average molecular weight expected for an equimolar mixture of V1 and Vh subunits (87 000–88 000). This suggests that little fractionation of the solution occurred at this speed. The solid curve in Figure 3 is drawn for a hypothetical ideal monomer-dimer equilibrium with a monomer molecular weight of 87 100 and an apparent formation constant of 5000 M^{-1} . The near fit of the data to this model suggests that the VI-Vh association is weak, since at least part of the association observed under these conditions is due to the V1 self-association.

Two methods that take account of the V1 self-association (with an assumed $K_{\text{V12}} = 5600 \text{ M}^{-1}$, Table I) have been used to estimate $K_{\text{VI-Vh}}$ in these solutions. The first method calculates $K_{\text{VI-Vh}}$ from an apparent K_1 by using the strategy described under Materials and Methods. The second method takes into account all of the species presumed to be present in the solution (V1, Vh, V1-V1, and V1-Vh) as fractional oligomers of the V1 subunit. Thus, the Vh subunit was treated as a 1.119-mer of the V1 subunit, with an association constant near 1, the V1-V1 dimer was assigned a stoichiometry of 2.00 and an association constant of 5600 M^{-1} , and the V1-Vh complex was considered a 2.119-mer of the V1 subunit with a formation constant that was to be determined. For both methods, the maximum

Table V: Factor Va Examined in 2 mM EDTA at 20 °C and at 15 000 rpm^a

method of analysis ^b	monomer mol wt	max concn (mM) ^c	K_{Vl-Vh} association (M^{-1}) ^d	rms (μm) ^e
app ideal monomer-dimer equilibrium	87 100 ^f	1.243	8800 (6400–12 000)	4.58
VI in ideal ^g equilibrium with Vh, VI-VI, and VI-Vh	82 500 ^f	1.398	9000 (6800–11 600)	4.57

^a Fit to data at a protein loading concentration of 0.065% with a maximum observed fringe displacement of 1.983 mm.

^b Stoichiometry of the model used to fit the data. ^c The data sets were edited so as to exclude the highest concentration data points. The maximum fringe displacement in the data set used for analysis is presented here. ^d Values for the VI-Vh association constant after correcting for the presence of a VI-VI association. See the text for the exact method used to obtain these values. ^e Root mean square of the variance for the nonlinear fit. ^f Value held constant during the nonlinear fit. ^g The VI subunit was considered to be in ideal equilibrium with a 1.119-mer (Vh subunit), a dimer (VI-VI), and a 2.119-mer (VI-Vh). See the text for details concerning the equilibrium constants assumed for each of these reactions.

Table VI: Sedimentation Coefficients and Frictional Coefficient Ratios for VI, Vh, and Factor Va

protein	addition to buffer A	$s_{20,w}^0$ (S)	f/f_{min}
VI	2 mM EDTA	$5.0_2 \pm 0.15$	1.38
Vh	2 mM EDTA	$5.2_9 \pm 0.16$	1.41
Va	2 mM EDTA	$5.2_5 \pm 0.2$	
Va	10 mM Ca^{2+}	$8.1_8 \pm 0.23$	1.39

concentration in the data sets was systematically decreased from 1.9 to 0.5 mM in increments of 0.1 mM, so as to minimize the contributions of higher polymers to the analyses. After each incremental decrease in the maximum concentration, the truncated data sets were fit by the two models. Table V presents the values for K_{VlVh} determined by the two methods outlined above. Association constants determined from experiments conducted at protein loading concentrations of 0.13% and 0.032% (data not shown) were in agreement (within 10%) with the values presented in Table V. Our best estimate of K_{VlVh} in 2 mM EDTA is $9400 M^{-1}$ (with a range from 6400 to 12 000 M^{-1}) on the basis of the data from three protein loading concentrations and as analyzed by both methods. This corresponds to a free energy of formation for the VIVh complex of -5.3 kcal/mol in 2 mM EDTA (at 20 °C), compared to the minimum free energy of -11.4 kcal/mol found for factor Va in 10 mM Ca^{2+} . Thus, it appears that Ca^{2+} has a very pronounced effect on K_{VlVh} .

It should be noted that the value of K_{VlVh} that we have determined in 2 mM EDTA may or may not be the same as that which would be found in a buffer that contained neither Ca^{2+} nor EDTA. There is some evidence that EDTA may not always be innocuous with regard to protein structure (Kronman & Bratcher, 1983), and both Greenquist & Colman (1975) and Hibbard & Mann (1980) have reported that there is an apparent interaction of EDTA with factor V. For this reason, it may not be prudent to determine the Ca^{2+} binding constant for factor Va on the basis of these data.

Sedimentation Coefficients of VI, Vh, and Va. The sedimentation coefficients for the VI subunit, the Vh subunit, and factor Va are presented in Table VI. The $s_{20,w}^0$ values for VI and Vh were the same when determined in a buffer that contained 10 mM Ca^{2+} rather than 2 mM EDTA. Neither

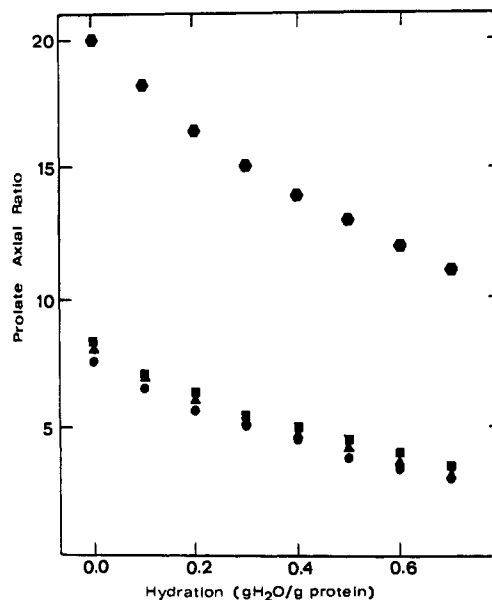


FIGURE 4: Prolate ellipsoid axial ratios of the VI, Vh, Va, and V molecules. Values of the prolate axial ratio were determined for each molecule at several degrees of hydration by using the procedure described under Materials and Methods. The axial ratios were determined by using the following values for molecular weights and sedimentation coefficients: for the VI subunit (\bullet), M_r 82 500 and $s_{20,w}^0 = 5.0_2$ S; for the Vh subunit (\blacksquare), M_r 92 300 and $s_{20,w}^0 = 5.2_9$ S; for the Va molecule (\blacktriangle), M_r 174 000 and $s_{20,w}^0 = 8.1_8$ S. The same procedure was used to compute axial ratios for factor V (\bullet) from the data of Nesheim et al. (1979a) (M_r 330 000, $s_{20,w}^0 = 9.1_9$ S).

the VI nor the Vh sedimentation coefficient changed significantly over the protein concentration range from 0.07 to 0.3%.

The sedimentation coefficient determined for factor Va dialyzed against buffer that contained 2 mM EDTA is close to that expected for a nonassociating mixture of VI and Vh subunits. Little or no change in this sedimentation coefficient was observed over the 0.07–0.3% concentration range. For factor Va dialyzed against buffer that contained 10 mM Ca^{2+} , we observed only one symmetrical (by eye) peak with a sedimentation coefficient of 8.2 S. A small change in the sedimentation coefficient (from 8.2 to 9.1 S) was observed over the concentration range from 0.07 to 0.54%. This change probably reflects an increase in the sedimentation coefficient due to the self-association of the Va molecules rather than a decrease in the sedimentation coefficient due to a dissociation of the Va molecule into subunits. The sedimentation equilibrium data support this view. On the basis of our values for K_{VlVh} in Va and the weaker Va dimer formation constant (Table IV), we estimate that more than 97% of the total protein will be in the form of a VI-Vh complex at a concentration of 0.01%. This value is less than the lowest concentration observed during these experiments. Nearly 10% of the protein will be in the form of a Va-Va dimer at a total protein concentration of 0.54%.

Calculated Hydrodynamic Parameters for VI, Vh, and Va. The sedimentation equilibrium molecular weights and the sedimentation coefficients presented previously have been used to determine both the frictional coefficients and the frictional coefficient ratios for the VI subunit, the Vh subunit, and the Va molecule. The frictional coefficient is 7.7×10^{-8} g/s for VI, 8.0×10^{-8} g/s for Vh, and 10.0×10^{-8} g/s for Va. The corresponding Stokes radii are 4.0 nm for VI, 4.1 nm for Vh, and 5.2 nm for Va. The frictional coefficient ratios presented in Table VI are consistent with proteins of moderate asymmetry. This asymmetry may account for the differences in the apparent molecular weights and the apparent Stokes radii

estimated by gel permeation chromatography of these molecules (Esmon, 1979). In Figure 4, we present estimates of the axial ratios for molecular models consisting of prolate ellipsoids of revolution at several levels of hydration. For comparison, we have treated the data of Nesheim et al. (1979a) for factor V in the same way and present these calculations in Figure 4.

Arrangement of the Subunits in Va. Comparison of the frictional coefficient ratios for the V_L, the V_H, and the Va molecules (Table VI) indicates that the association of the V_L and V_H subunits does not create a molecule of greater apparent asymmetry than either of the two subunits. For the prolate ellipsoid of revolution model, this corresponds to a side by side arrangement of the subunits rather than an end to end arrangement. Assuming that the molecules are prolate ellipsoids with a level of hydration of 0.3 g of H₂O/g of protein, and using our values for the partial specific volumes and axial ratios, the major and minor semiaxis lengths would be 8.4×1.7 nm for V_L, 9.3×1.7 nm for V_H, and 11.0×2.1 nm for factor Va.

Hydrodynamic Differences between Factor V and Factor Va. The pronounced difference in the hydrodynamic properties of factor V and factor Va (illustrated in Figure 4) suggests that the presence of the activation peptide (Esmon, 1980) strongly influences the hydrodynamic behavior of factor V. In order to account for the observed differences, either (1) the presence of the activation peptide must cause structural asymmetry in factor V or (2) the activation region must bind over 5 g of H₂O/g of protein. While it is possible that the activation region may bind more than 0.3 g of H₂O/g of protein because of its high carbohydrate content (Esmon, 1980), it is doubtful that the levels of hydration would reach 5 g of H₂O/g of protein. It appears, then, that the activation peptide is responsible for much of the asymmetry observed for the factor V molecule. The amino acid composition, the high carbohydrate content, and the presumed high asymmetry of the activation peptide are consistent with a factor V structure in which the activation peptide resembles a long tail projecting from the more globular V_H and V_L regions at the amino and carboxy ends of the molecule (Esmon, 1980; Fass et al., 1983).

Conclusions

Our results suggest that several equilibria should be considered (e.g., $V_L + V_H \leftrightarrow V_a$, $V_L + V_L \leftrightarrow V_{L_2}$, $V_a + V_a \leftrightarrow V_{a_2}$) when interpreting data involving factor Va and its role in the prothrombinase complex. The results presented in Tables I–V provide estimates for several of these equilibria.

Of particular interest is the apparent association of Va molecules to form dimers. This equilibrium has an apparent dimer formation constant of 3100 M^{-1} , corresponding to a free energy of association of -4.6 kcal/mol at 20°C . This dimer formation constant is consistent with a mechanism in which the Va self-association is mediated through V_L subunit contacts. Although the association constant for the formation of Va dimers is small, the concentration of factor Va localized on membrane surfaces (both in vivo and in vitro) may be high enough for Va multimers to form. The formation of higher complexes would have interesting consequences regarding the structure, kinetics, and regulation of the prothrombinase complex.

Acknowledgments

We thank Eric Wassilak and Julie Saugstad for their excellent technical assistance in the protein purification. We also thank Dr. Diana Lee of the Oklahoma Medical Research Foundation for allowing us to use their model E ultracentrifuge

for the sedimentation velocity experiments. The generous provision of computer time by the University of Connecticut and the University of Oklahoma computer facilities is deeply appreciated.

Registry No. Blood coagulation factor Va, 65522-14-7; calcium, 7440-70-2.

References

- Ansevin, A. T., Roark, D. E., & Yphantis, D. A. (1970) *Anal. Biochem.* **34**, 237–261.
- Cantor, C. R., & Schimmel, P. R. (1980) in *Biophysical Chemistry*, Part II, pp 560–569, W. H. Freeman, San Francisco, CA.
- Cohn, E. J., & Edsall, J. T. (1943) in *Proteins, Amino Acids and Peptides as Ions and Dipolarions*, p 374, Reinhold, New York.
- Correia, J. C. (1981) Ph.D. Dissertation, University of Connecticut, Storrs, CT.
- Dahlback, B. (1980) *J. Clin. Invest.* **66**, 583–591.
- Davie, E. W., & Fujikawa, K. (1975) *Annu. Rev. Biochem.* **44**, 799–829.
- Esmon, C. T. (1979) *J. Biol. Chem.* **254**, 964–973.
- Esmon, C. T. (1980) in *The Regulation of Coagulation* (Mann, K. G., & Taylor, F. B., Eds.) pp 137–143, Elsevier/North-Holland, New York.
- Fass, D., Hewick, R., Knutson, G., Nesheim, M., & Mann, K. (1983) *Thromb. Haemostasis* **50**, 255a.
- Greenquist, A. C., & Colman, R. W. (1975) *Blood* **46**, 769–782.
- Guinto, E. R. (1983) Ph.D. Dissertation, The University of Oklahoma Health Sciences Center, Oklahoma City, OK.
- Guinto, E. R., & Esmon, C. T. (1982) *J. Biol. Chem.* **257**, 10038–10043.
- Hibbard, L. S., & Mann, K. G. (1980) *J. Biol. Chem.* **255**, 638–645.
- Jackson, C. M., & Nemerson, Y. (1980) *Annu. Rev. Biochem.* **49**, 765–811.
- Johnson, M. L., Correia, J. C., Yphantis, D. A., & Halvorson, H. R. (1981) *Biophys. J.* **36**, 575–588.
- Kane, W. H., & Majerus, P. W. (1981) *J. Biol. Chem.* **256**, 1002–1007.
- Kronman, M. J., & Bratcher, S. C. (1983) *J. Biol. Chem.* **258**, 5707–5709.
- Laemmli, U. K. (1970) *Nature (London)* **227**, 680–685.
- Laue, T. M. (1981) Ph.D. Dissertation, University of Connecticut, Storrs, CT.
- Laue, T. M., & Yphantis, D. A. (1979) *Biophys. J.* **25**, 164a.
- McMeekin, T. L., & Marshall, K. (1952) *Science (Washington, D.C.)* **116**, 142–143.
- Nesheim, M. E., & Mann, K. G. (1979) *J. Biol. Chem.* **254**, 1326–1334.
- Nesheim, M. E., Myrmel, K. H., Hibbard, L., & Mann, K. G. (1979a) *J. Biol. Chem.* **254**, 508–517.
- Nesheim, M. E., Taswell, J. B., & Mann, K. G. (1979b) *J. Biol. Chem.* **254**, 10952–10962.
- Nesheim, M. E., Hibbard, L. S., Tracy, P. B., Bloom, J. W., Myrmel, K. H., & Mann, K. G. (1980) in *The Regulation of Coagulation* (Mann, K. E., & Taylor, F. B., Eds.) pp 145–159, Elsevier/North-Holland, New York.
- Paul, C. H., & Yphantis, D. A. (1972) *Anal. Biochem.* **48**, 588–604.
- Roark, D. E., & Yphantis, D. A. (1969) *Ann. N.Y. Acad. Sci.* **164**, 245–278.
- Rosing, J., Tans, G., Govers-Riemslog, J. W. P., Zwaal, R. F. A., & Hemker, H. C. (1980) *J. Biol. Chem.* **255**, 274–283.

- Schachman, H. K. (1959) *Ultracentrifugation in Biochemistry*, p 82, Academic Press, New York.
- Sober, H. A., Ed. (1970) *Handbook of Biochemistry*, 2nd ed., pp C-67-69, Chemical Rubber Publishing Co., Cleveland, OH.
- Squire, P. G., & Li, C. H. (1961) *J. Am. Chem. Soc.* 83, 3521-3528.
- Tanford, C. (1961) *Physical Chemistry of Macromolecules*, pp 194-233, Wiley, New York.
- Teller, D. C. (1973) *Methods Enzymol.* 27, 346-441.
- Teller, D. C., Horbett, T. A., Richards, E. G., & Schachman, H. K. (1969) *Ann. N.Y. Acad. Sci.* 64, 66-101.
- Van Holde, K. E., & Baldwin, R. I. (1958) *J. Phys. Chem.* 62, 734-743.
- Washburn, E. W., Ed. (1928) *International Critical Tables of Numerical Data, Physics, Chemistry and Technology*, Vol. 3, McGraw-Hill, New York.
- Weast, R. C., Ed. (1968) *Handbook of Chemistry and Physics*, 49th ed., Chemical Rubber Publishing Co., Cleveland, OH.
- Weber, G. (1975) *Adv. Protein Chem.* 29, 1-83.
- Yphantis, D. A. (1964) *Biochemistry* 3, 297-317.
- Yphantis, D. A., & Waugh, D. F. (1956) *J. Phys. Chem.* 60, 623-629.
- Yphantis, D. A., Correia, J. J., Johnson, M. L., & Wu, G.-M. (1978) in *Physical Aspects of Protein Interactions* (Castimpoalas, N., Ed.) pp 275-303, Elsevier/North-Holland, New York.

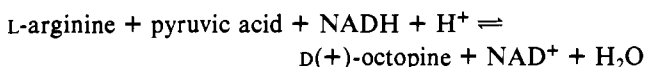
Octopine Dehydrogenase from *Pecten maximus*: Steady-State Mechanism[†]

Jeffrey L. Schrimsher[‡] and Kenneth B. Taylor*

ABSTRACT: The steady-state kinetic mechanism of the reaction catalyzed by octopine dehydrogenase [*N*²-(1-carboxyethyl)-L-arginine:NAD⁺ oxidoreductase] was investigated at pH 6.9 and 9.2 by studies of substrate inhibition, analogue inhibition, and product inhibition. In the direction of octopine synthesis, the inhibition patterns in the presence of δ -guanidinovalerate and propionate show that NADH binds to the enzyme first followed by L-arginine and pyruvate which bind randomly. In the direction of octopine oxidation, the substrate patterns show

that NAD binds to the enzyme before octopine in a rapid equilibrium fashion, and the product inhibition patterns show that the products L-arginine and pyruvate are released in a random fashion. Double, synergistic, substrate inhibition by L-arginine and pyruvate was shown to be due to binding (hypothetically of the imine) to the free enzyme and the enzyme-NAD complex. Furthermore, an alternate minor pathway was demonstrated which includes an enzyme-NADH-octopine complex and an enzyme-octopine complex.

Octopine dehydrogenase from *Pecten maximus* (EC 1.5.1.11) catalyzes the reaction



The enzyme is a monomer with a molecular weight of 38 000 (Thoai et al., 1969), and although it lacks any metal or flavin (Thoai et al., 1969; Pho et al., 1970), it contains a prosthetic group involved in electron transfer (J. L. Schrimsher and K. B. Taylor, unpublished results) whose structure is not presently known.

Several kinetic studies of octopine dehydrogenase have been undertaken (Doublet & Olomucki, 1975; Monneuse-Doublet et al., 1978), but these studies were limited by substrate inhibition to a rather narrow range of substrate concentrations and lacked the use of statistical analysis of data.

Octopine dehydrogenase has also been shown to exhibit substrate inhibition by L-arginine and pyruvate as well as octopine [(*R*)-*N*²-(1-carboxyethyl)-L-arginine] (Monneuse-Doublet et al., 1978). However, the mechanism of the substrate inhibition was not examined.

The following reports our investigation on the nature of the substrate inhibition induced by L-arginine and pyruvic acid, the mechanism of several reversible, analogue inhibitors, and

the steady-state kinetic mechanism of octopine dehydrogenase from *Pecten maximus*.

Experimental Procedures

Materials. L-Arginine hydrochloride, sodium pyruvate, NAD, and NADH were from Sigma Chemical Co. Propionic acid was from J. T. Baker Chemical Co. D(+)-Octopine was a generous gift of Dr. Leo Hall, University of Alabama in Birmingham.

Octopine dehydrogenase from *Pecten maximus*, obtained as a dry powder from Sigma Chemical Co., had a specific activity of 11.2 units/mg of protein. The results of polyacrylamide gel electrophoresis indicate that the enzyme preparation is homogeneous (J. L. Schrimsher and K. B. Taylor, unpublished results).

Preparation of Inhibitors. δ -Guanidinovalerate was prepared from δ -aminovalerate (3.1 g) according to the procedure described by Kurtz (1949) for the synthesis of arginine from ornithine except that the steps for the protection of the α -amine were excluded. The pH of the solution containing the product was adjusted to 1.0 with HCl, and the solution was applied (1 mL/min, 55 mL) to a column (1.6 \times 13 cm) of Dowex 50W-X8 (H⁺ form). The column was developed with 0.1 M ammonia, and the effluent that contained product [detected according to the procedure of Otten & Schilperoort (1977)] was dried in vacuo. The product (2.3 g) was recrystallized twice from water (20 mL). *N*²-Ethyl-L-arginine was synthesized from L-arginine and acetaldehyde according to the procedure of Biellmann et al. (1977) for reductive amination

[†] From the Department of Biochemistry, University of Alabama in Birmingham, Birmingham, Alabama 35294. Received August 25, 1983.

[‡] Present address: Department of Biochemistry, University of Wisconsin, Madison, WI 53706.